Available online at www.sciencedirect.com

SciVerse ScienceDirect

Ceramics International 39 (2013) 4299–4305

CERAMICS INTERNATIONAL

www.elsevier.com/locate/ceramint

Atomic structure and chemistry of dense nano-precipitates in MgB_2 ceramic

Xueyan Song*

Department of Mechanical and Aerospace Engineering, West Virginia University, Morgantown, WV 26506, USA

Received 1 October 2012; received in revised form 5 November 2012; accepted 6 November 2012
Available online 13 November 2012

Abstract

Ceramic MgB_2 superconductor has great potential for applications in the devices. Doping MgB_2 with carbon or SiC has been successful in improving critical current density J_c, the upper critical field H_{c2} and flux-pinning. However, the presence of nano-precipitates, and their microstructure and chemistry, upon alloying/doping MgB_2 grains are largely unexplored. In this paper, the atomic structure and chemistry of 5–10 nm dense nano-precipitates were discovered in purified MgB_2 pellets by removing B_2O_3. The nano-precipitates are platelet-shaped and fully coherent with the MgB_2 grains and having the longer axis of the plate perpendicular to the *c*-axis of MgB_2 grains. Systematic conventional and analytical Transmission Electron Microscopy (TEM) was carried out to study the atomic structure and chemistry of those nano-precipitates. The practical experimental approach of optimizing the composition and synthesis heat treatment of MgB_2 to induce dense uniformly distributed nano-precipitates is also discussed.

Keywords: B. Electron microscopy; B. Inclusion; C. Superconductivity; MgB_2

1. Introduction

MgB_2 superconductor, with superconducting temperature T_c of 39 K, has great potential for application in the electric power transportation and devices. Because the grain boundaries (GBs) do not block current flow [1,2] as they do in the high temperature superconductors (HTS), the technological barriers to MgB_2 conductor fabrication are very much less than that for HTS [3,4]. But in the MgB_2 material, the critical current density (J_c) drops rapidly with increasing magnetic field strength [5]. One of the practical challenges of the development of MgB_2 superconducting wires is to improve the J_c. The magnitude and field dependence of the critical current are related to the presence of structural defects, which can 'pin' the quantized magnetic vortices that permeate the material. Currently, J_c of MgB_2 is severely affected by the materials microstructure issues such as the high porosity, bad GB-connectivity and the lack of the crystal defects that could act as flux-pinning centers within the MgB_2 grains. Accordingly, one critical challenge for development of high performance MgB_2 is to understand and to optimize the flux pinning in MgB_2.

Various research have been attempted to improve the flux pinning for MgB_2, such as irradiation [6], chemical doping [7] and reducing the grain size [8,9]. MgB_2 is clearly able to incorporate a variety of nanoscale pins, such as MgO [10], SiC-doping [11], and Y_2O_3-doping [12], with significant improvement of bulk pinning. However, the practical difficulty of incorporating nanoparticles in the MgB_2 is that adding those materials will increase the normal state resistivity, and those added materials often end up sitting in the GBs of MgB_2 and reduce the active cross-section of carrying the super-current [13–15]. Their influence of blocking the current can easily exceed the benefits of having effective pinning centers in high fields.

By contrast, inducing the dense uniformly distributed nano-precipitates into the MgB_2 grains, without having the accumulation of the precipitates at the MgB_2 GBs would be an ideal case for improving the flux pinning properties. Precipitates in a superconductor can pin vortices [16–19] by reduction or suppression of the condensation energy within their volume, and more indirectly by creating defects such as stacking faults, dislocations in the superconducting matrix.

*Tel.: +1 304 293 3269; fax: +1 304 293 6689.
E-mail address: xueyan.song@mail.wvu.edu

0272-8842/$ - see front matter © 2012 Elsevier Ltd and Techna Group S.r.l. All rights reserved.
http://dx.doi.org/10.1016/j.ceramint.2012.11.011

For effective pinning centers, the size and the separation of the foreign particles are critical [20]. For example, pinning centers in conventional methods of fabrication of low T_c superconductors are developed by modifying the thermomechanical processing. Finely dispersed nano-sized non-superconducting Ti phase precipitated during heat treatment is strong flux pinners in NbTi. For effective pinning the typical thickness of the α-Ti phase must be 1–4 nm with a separation of 5–20 nm [21,22]. For HTS $YBa_2Cu_3O_{7-x}$ (YBCO) coated conductors, both microstructural and electromagnetic evidences were found for an enhanced vortex pinning in Sm substituted coated conductors which produces 17 vol% of mixed $(Y,Sm)_2O_3$ nano-precipitates that are ~10 nm in size and separated by ~15 nm. Such precipitate arrays can be a powerful way to enhance the critical current density J_c and high-field performance of YBCO coated conductors [23]. By similar approach, for having the strong flux pining in MgB_2, the intragranular nano-precipitates should be dense and with the size comparable to the MgB_2 superconducting coherence length of 5–12 nm [4,20]. However, for the MgB_2, the production of dense uniformly distributed nano-precipitates remains challenging in MgB_2 synthesized in any form, such as bulk, thin film and wires. The presence of nano-precipitates, and their microstructure and chemistry, upon alloying/doping MgB_2 grains are largely unexplored.

In this paper, the dense and evenly distributed nano-precipitates are found in the bulk scale MgB_2 ceramic samples. The atomic structure and chemistry of the precipitates were analyzed using advanced TEM. The practical experimental approach of optimizing the composition and synthesis heat treatment of MgB_2 to induce dense uniformly distributed nano-precipitates, and the effect of such precipitates on the electromagnetic properties and application of MgB_2 is discussed.

2. Experimental details

As-received amorphous B powder (Alfa-Aesar 99%) was pressed into 8–10 mm diameter pellets by cold isostatic pressing, and then heat treated at 950 °C for 48 h in flowing 4% H_2 in Ar in order to remove B_2O_3. Such pellets were reacted at 950 °C for 24 h with Mg vapor to form MgB_2. The synthesis and processing procedure of the MgB_2 pellets were detailed in a paper [24]. In this paper, the detailed TEM analysis is presented on the morphology, distribution, atomic structure and chemistry of the nano-precipitates found in those purified MgB_2 samples.

Samples for TEM were prepared by mechanical polishing and ion milling. Diffraction contrast and high-resolution TEM (HRTEM) investigations were performed using a microscope (Philips CM200) operated at 200 kV with point resolution of 0.19 nm. High-angle annular dark-field (HAADF) *Z*-contrast imaging in a scanning TEM (STEM) was performed using a 200 kV (JEOL 2010F) microscope focused to a ~0.14 nm diameter electron probe with the inner cut-off angle of the HAADF detector > 52 mrad. The nanoscale chemistry was analyzed using a 0.2 nm probe and on-axis electron energy loss spectroscopy (EELS) with an energy dispersion of 0.2 eV per channel and an energy resolution of 1.0 eV in a JEOL 2010F STEM.

3. Results and discussion

3.1. Morphology and crystallographic features of precipitates in the MgB_2 grains

The electron diffraction contrast images taken from the MgB_2 grains in Fig. 1 shows that the MgB_2 grains are with size of microns. There are pores with the size 100–200 nm. Some of the pores are faceted. There are spherical MgO particles with the size of 40 nm or bigger within the MgB_2 grains. Pores and MgO particles are commonly observed in the MgB_2 film, wire and bulk samples. The unique feature of this sample is found when the electron beam is imaging along the [100] direction of MgB_2 grains. Diffraction contrast images under higher magnification in Fig. 2 shows the uniform distribution of dense nano-precipitates. The precipitates are platelet-shaped with the size of 5–15 nm in longer axis and 2–5 nm in the shorter axis. The nano-precipitates are with well-defined crystallography relationship with the MgB_2 matrix and the longer axis of the nano-precipitates is lying on the basal plane of the hexagonal MgB_2 lattice. HRTEM images taken from the [100] zone axis of MgB_2 grains in Fig. 3 confirm that the platelet precipitates all lie with their long axis perpendicular to the [001] direction of MgB_2 grains. The HRTEM images also show the precipitates have the same lattice fringes as the MgB_2 matrix except for having the periodic contrast modulating along the [001] direction of the MgB_2. The modulation period of nano-precipitates is twice of the MgB_2 lattice constant along the *c*-axis. In consistent with the image contrast, the corresponding Fourier transformation from the area containing nano-precipitates (Fig. 3a)

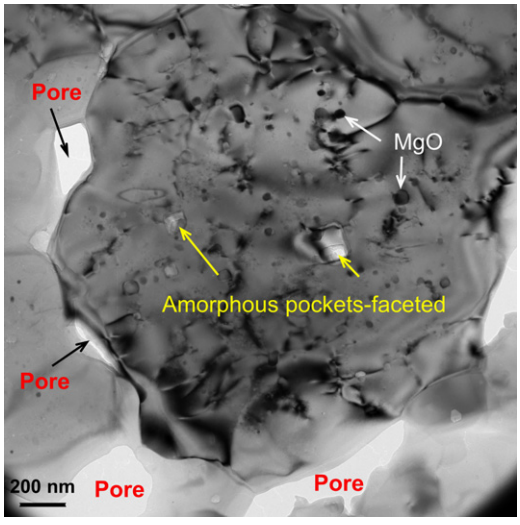

Fig. 1. TEM diffraction contrast images revealing the morphology of large MgB_2 grains, amorphous pockets and some spherical shaped MgO particles.

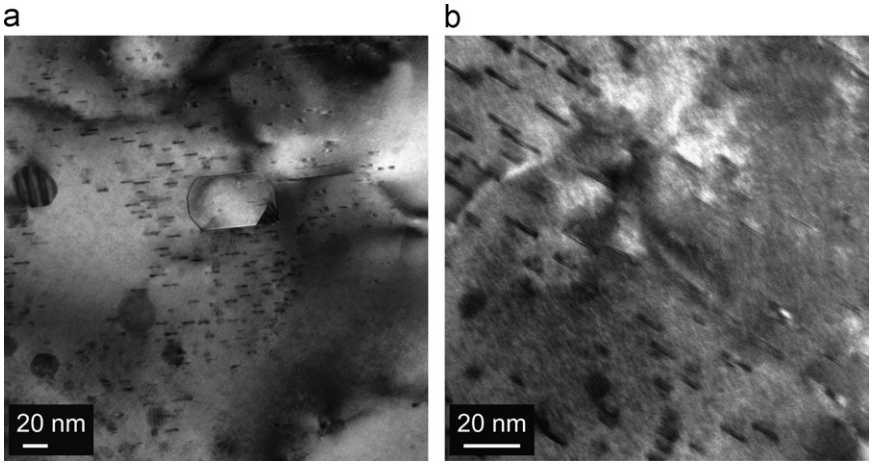

Fig. 2. TEM diffraction contrast images showing the morphology and distribution of the nano-precipitates. Images (a) and (b) were taken from different regions.

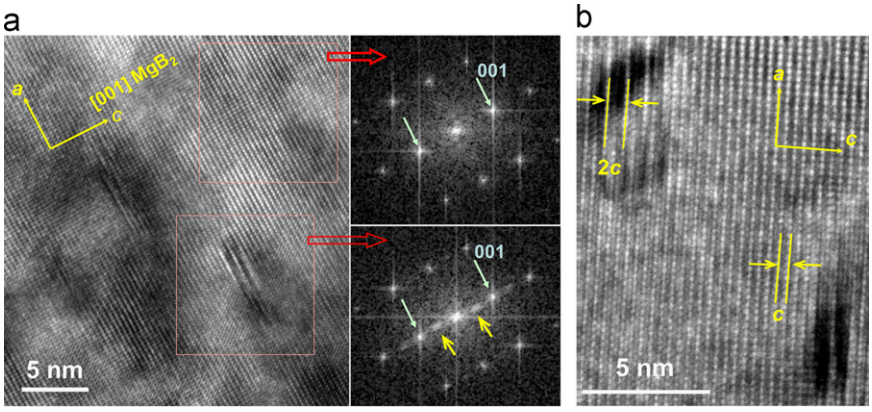

Fig. 3. (a) HREM images and corresponding Fourier transformation of the nano-precipitates and (b) high resolution images showing the contrast modulation in the precipitates.

shows the extra diffraction spots along the [001] direction with a vector equal to ½[001]. Because of the nano-precipitates are having the structure modulation along the [001] direction of MgB_2 lattice, under TEM, the contrast of nano-precipitates is pronounced only as the incident electron direction is close to the [100] direction of MgB_2. Under TEM, over several tens of MgB_2 grains were studied to exam the commonality of the existence of such precipitates. It was found that as long as the [100] direction MgB_2 grains are tilted to be parallel to the electron beam, the dense nano-precipitates are observed. Accordingly, it is believed that the existence of nano-precipitates in the MgB_2 grain is common structural feature of the entirely purified MgB_2 polycrystalline samples [24].

3.2. Atomic structure and chemistry of precipitates

The atomic structure of the precipitates was imaged using STEM equipped with both the bright field and HAADF detector. The bright field images and the HAADF *Z*-contrast images are taken simultaneously. The bright field STEM image in Fig. 4(a and b) clearly shows the precipitates. By contrast, the corresponding HAADF *Z*-contrast images in Fig. 4(c) did not show any contrast from the precipitates. In the HAADF *Z*-contrast images taking along the [100] directions of MgB_2, the bright columns are corresponding to the Mg columns. By contrast, the B atoms are not visible due to the low scattering amplitude of B atoms. Since the HAADF images did not show the contrast difference between the MgB_2 bulk and nano-precipitates, it clearly indicated that nano-precipitates are having the same Mg atom arrangements as that for MgB_2 bulk, and the structure modulation in the *c*-direction of the precipitates probably originates from the structure and chemistry changes in the Boron lattices, which are not shown in the *Z*-contrast images at all.

To reveal the chemistry of the nano-precipitates, the EELS was taken from the precipitates and the MgB_2 grains. Only Mg, B and O were identified in the precipitates, and only Mg and B were found in the MgB_2 grains. No other elements were present in the sample. Boron K-edge EELS spectra taken from the nano-precipitates

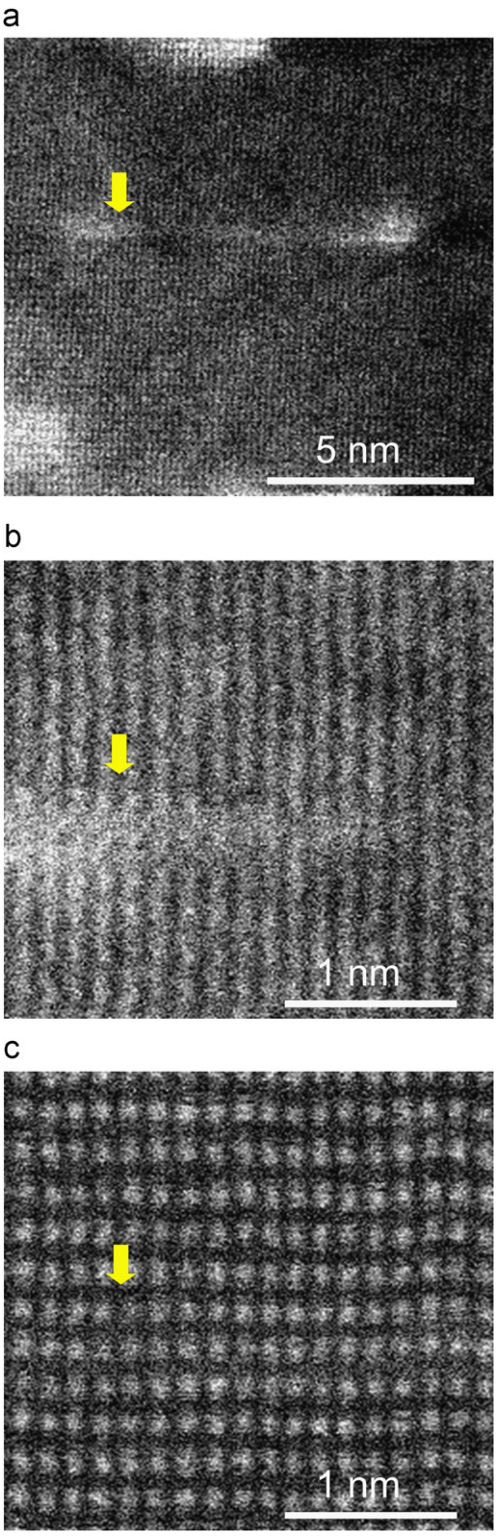

Fig. 4. STEM images of the precipitates, indicated by the arrow: (a) low magnification bright-field images; (b) high magnification of BF-STEM images and (c) simultaneous HAADF image corresponding to (b).

and bulk are shown in Fig. 5. The EELS is processed for background subtraction and corrected for multiple-scattering contributions. It can be seen the near edge fine structure of EELS from the precipitates are different from

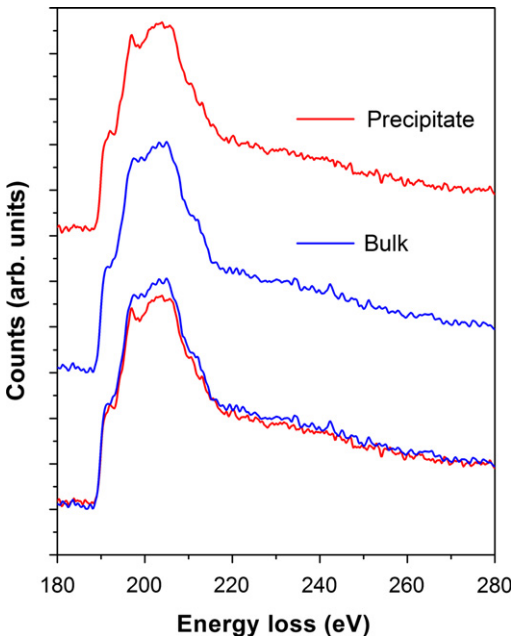

Fig. 5. EELS of boron K-edge of precipitates and bulk MgB_2.

that of the bulk and the pre-peak intensity of the boron K-edge spectra of nano-precipitates is slightly higher than that of the MgB_2. The EELS spectra from oxygen K-edge of the nano-precipitates, shown in Fig. 6, also indicate the significant amount of oxygen in the nano-precipitates. By contrast, the intensity of oxygen K-edge EELS from MgB_2 matrix is very low. The above results show that the composition of the nano-precipitates is $Mg(BO)_x$ phases. Because the HRTEM images and FFT results show that the nano-precipitates lattices are having the structure/chemistry modulation with period twice of the MgB_2 lattice constant along the *c*-axis, in combination with the *Z*-contrast and EELS results, it is reasonable to assume that, the nano-precipitates are having the oxygen ordering every other B lattices along the *c*-axis of MgB_2 grains. Nevertheless, because *Z*-contrast imaging was not able to resolve the boron and oxygen atoms, it is unclear about the exact atomic positions that oxygen incorporate into the boron lattice.

3.3. Formation of nano-precipitates and approach of introducing different defects into MgB_2

The integrated TEM, HREM, *Z*-contrast STEM imaging and EELS carried out on the precipitates have indicated the composition of nano-precipitates as $Mg(BO)_x$. In the meanwhile, it is believed that MgB_2 grains are free or with very tiny amount of oxygen, which is evidenced by the EELS spectrum and by the high T_c of 38.5 K, measured for the sample [24]. In the meanwhile, the oxygen contamination in the starting materials is regarded as the source of having dense nano-precipitates. In the present study, those $Mg(BO)_x$ precipitate sizes are comparable with the DyB_4 precipitates [25] that acts as the effective pinning centers for enhancing

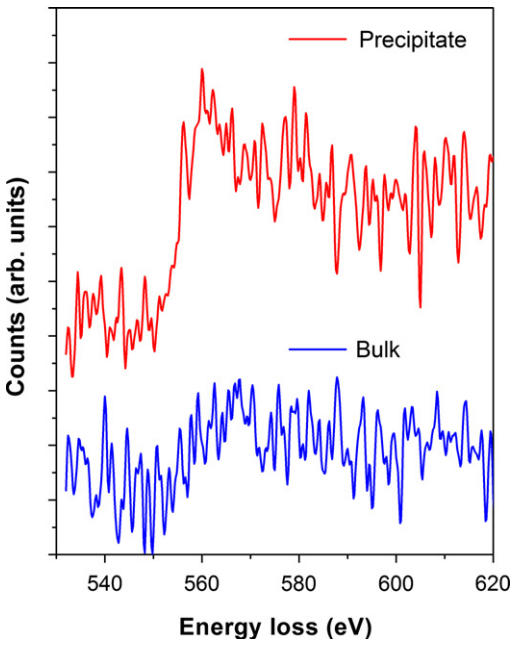

Fig. 6. EELS of oxygen K-edge of precipitates and bulk MgB_2.

the critical current density. For the MgB_2, the coherence length values along the *ab*-plane range between 3.7 and 12.8 nm and along the *c*-axis between 1.6 and 5.0 nm. Dense nano-precipitates with the size of 5–15 nm in longer axis and 2–5 nm in the shorter axis, comparable with the superconducting coherence length 5–12 nm for MgB_2, could act as very effective flux-pinning centers under high magnetic field.

The presence of such dense precipitates in the bulk MgB_2 samples are very intriguing. Significant effort has also been put to investigate the effect of oxygenation on the superconducting properties of MgB_2 and it is found that MgB_2 are remarkably stable against damage from oxygen [26]. The author in this paper had also investigated many MgB_2 samples using TEM before [10,12,27–30]. Those samples are usually with MgO particles and definitely no plate-shaped nano-precipitates. Interestingly, in the present study, TEM results indicated that the existence of nano-precipitates in the MgB_2 grain is common structural feature of the entire polycrystalline MgB_2 samples that we previously synthesized. It must be pointed out that, for the present study, the nano-precipitates in the samples prepared in the attempt of removing the B_2O_3 impurities in the starting precursor materials. Those starting precursor materials of boron powders were initially processed by "heat treated at 950 °C for 48 h in flowing 4% H_2 in air in order to remove B_2O_3". X-ray diffraction and microstructure analysis show that removing B_2O_3 results in a decrease in MgO from 5.3 to 1.5 mol% in the final reacted MgB_2 [24]. It is from those samples that made from starting boron powders subjected to B_2O_3 purification; such dense nano-precipitates were found. Accordingly, it is thus believed there is a "fine range" of oxygen concentration in the starting precursor materials to render the formation of the nano-precipitates without forming the large dispersed MgO particles.

Unlike the dispersed large MgO particles in the MgB_2 matrix [24], the nano-precipitates are having well-defined orientation relationship with MgB_2 matrix, and having their longer axis of platelet perpendicular to the *c*-axis of MgB_2 matrix, and oxygen order every other unit cell in the *c*-direction of MgB_2 lattice. In other words, during the MgB_2 reactions, the oxygen goes into the MgB_2 lattice as impurity by forming oxygen point defects in the B site and leaving the Mg site un-disturbed. Those oxygen impurity atoms accumulate at the scale of several nanometers and order every other unit cell in the *c*-direction of MgB_2 lattice. Thus, heat-treatment conditions that promote the oxygen atoms going into the MgB_2 lattice and subsequently ordering is the key. As a fact, this is fully consistent with the conclusion by Kovac et al. [31] in stating that "the level of MgO should be optimized as a compromise between inter-grain connectivity and introducing pinning centers". Furthermore, the present study provides the microstructure evidence of existence of dense nano-precipitates $Mg(BO)_x$ and their atomic structure.

By contrast to the precipitates, the EELS results have demonstrated that MgB_2 grain matrix as shown in Fig. 2 is free or with very tiny amount of oxygen. EELS did not show any trace of carbon contamination in the MgB_2 grains. The clean MgB_2 grain matrix provides possibility of having additional defects in the MgB_2. The synergetic combination of "Nano-precipitates in the MgB_2 grain" and "Point defects such as carbon impurity in the MgB_2 lattice" will be very possible and interesting. Recently, synergetic combination of different types of defects to optimize the pinning landscape of HTS YBCO, has been proved to be very successful and produces thick films with remarkable critical current [32]. For MgB_2, the pinning provided by intragruanular nano-precipitates, C substitution in MgB_2 lattice may take place at the same time at superconducting temperatures, resulting in a synergetic combination of optimal defects from all sources. A full understanding of the way to control the formation of the above mentioned different defects in MgB_2 will guide future technological development of MgB_2 for commercial exploitation.

4. Summary

Dense platelet shaped nano-precipitates with the size of 5–10 nm were found in the MgB_2 bulk samples. The nano-precipitates are fully coherent with the MgB_2 grains and having the longer axis of the plate perpendicular to the *c*-axis of MgB_2 grains. Under TEM, the precipitates show the periodic contrast modulating along the [001] direction of the MgB_2. The modulation period of nano-precipitates is twice of the MgB_2 lattice constant along the *c*-axis. Using the combination of atomic resolution bright field, dark field STEM imaging, and EELS, the composition of the precipitates were identified as $Mg(BO)_x$. The oxygen is

assumed to substitute B and form ordering every other B lattices along the *c*-axis of MgB_2 grains. The precipitates are common feature of the samples investigated. It is from those samples that made from starting boron powders subjected to B_2O_3 purification; such dense nano-precipitates were found. Accordingly, it is thus believed there is a "fine range" of oxygen concentration in the starting precursor materials to render the formation of the nano-precipitates without forming the large dispersed MgO particles. The nano-precipitates with the size of 5–15 nm longer axis and 2–5 nm in the shorter axis could be very effective pinning centers. With the presence of nano-precipitates, the MgB_2 grains are free of oxygen. The clean MgB_2 lattice provides possibility of having point defects to further enhance the flux pinning properties. The synergetic combination of "nano-precipitates in the MgB_2 grain" and "point defects such as carbon impurity in the MgB_2 lattice" is suggested for increasing the critical current density of MgB_2.

Acknowledgment

The great support and effort from Prof. David Larbalestier for this work are highly appreciated. The author thanks Prof. Eric Hellstrom and Dr. Jiangyi Jiang for the very helpful discussions.

References

[1] D.C. Larbalestier, L.D. Cooley, M.O. Rikel, A.A. Polyanskii, J. Jiang, S. Patnaik, X.Y. Cai, D.M. Feldmann, A. Gurevich, A.A. Squitieri, M.T. Naus, C.B. Eom, E.E. Hellstrom, R.J. Cava, K.A. Regan, N. Rogado, M.A. Hayward, T. He, J.S. Slusky, P. Khalifah, K. Inumaru, M. Haas, Strongly linked current flow in polycrystalline forms of the superconductor MgB_2, Nature 410 (6825) (2001) 186–189.

[2] A.A. Polyanskii, A. Gurevich, J. Jiang, D.C. Larbalestier, S.L. Bud'ko, D.K. Finnemore, G. Lapertot, P.C. Canfield, Magneto-optical studies of the uniform critical state in bulk MgB_2, Superconductor Science and Technology 14 (10) (2001) 811–815.

[3] P. Grant, Superconductivity—rehearsals for prime time, Nature 411 (6837) (2001) 532–533.

[4] D. Larbalestier, A. Gurevich, D.M. Feldmann, A. Polyanskii, High T_c superconducting materials for electric power applications, Nature 414 (6861) (2001) 368–377.

[5] P. Vase, R. Flukiger, M. Leghissa, B. Glowacki, Current status of high-T_c wire, Superconductor Science and Technology 13 (7) (2000) R71–R84.

[6] Y. Bugoslavsky, L.F. Cohen, G.K. Perkins, M. Polichetti, T.J. Tate, R. Gwilliam, A.D. Caplin, Enhancement of the high-magnetic field critical current density of superconducting MgB_2 by proton irradiation, Nature 411 (6837) (2001) 561–563.

[7] Y. Zhao, Y. Feng, C.H. Cheng, L. Zhou, Y. Wu, T. Machi, Y. Fudamoto, N. Koshizuka, M. Murakami, High critical current density of MgB_2 bulk superconductor doped with Ti and sintered at ambient pressure, Applied Physics Letters 79 (8) (2001) 1154–1156.

[8] E. Martinez, P. Mikheenko, M. Martinez-Lopez, A. Millan, A. Bevan, J.S. Abell, Flux pinning force in bulk MgB_2 with variable grain size, Physical Review B 75 (13) (2007).

[9] A. Gumbel, J. Eckert, G. Fuchs, K. Nenkov, K.H. Muller, L. Schultz, Improved superconducting properties in nanocrystalline bulk MgB_2, Applied Physics Letters 80 (15) (2002) 2725–2727.

[10] C.B. Eom, M.K. Lee, J.H. Choi, L.J. Belenky, X. Song, L.D. Cooley, M.T. Naus, S. Patnaik, J. Jiang, M. Rikel, A. Polyanskii, A. Gurevich, X.Y. Cai, S.D. Bu, S.E. Babcock, E.E. Hellstrom, D.C. Larbalestier, N. Rogado, K.A. Regan, M.A. Hayward, T. He, J.S. Slusky, K. Inumaru, M.K. Haas, R.J. Cava, High critical current density and enhanced irreversibility field in superconducting MgB_2 thin films, Nature 411 (6837) (2001) 558–560.

[11] S.X. Dou, V. Braccini, S. Soltanian, R. Klie, Y. Zhu, S. Li, X.L. Wang, D. Larbalestier, Nanoscale-SiC doping for enhancing J_c and H_{c2} in superconducting MgB_2, Journal of Applied Physics 96 (12) (2004) 7549–7555.

[12] J. Wang, Y. Bugoslavsky, A. Berenov, L. Cowey, A.D. Caplin, L.F. Cohen, J.L.M. Driscoll, L.D. Cooley, X. Song, D.C. Larbalestier, High critical current density and improved irreversibility field in bulk MgB_2 made by a scalable, nanoparticle addition route, Applied Physics Letters 81 (11) (2002) 2026–2028.

[13] J.M. Rowell, The widely variable resistivity of MgB_2 samples, Superconductor Science and Technology 16 (6) (2003) R17–R27.

[14] J.M. Rowell, S.Y. Xu, H. Zeng, A.V. Pogrebnyakov, Q. Li, X.X. Xi, J.M. Redwing, W. Tian, X.Q. Pan, Critical current density and resistivity of MgB_2 films, Applied Physics Letters 83 (1) (2003) 102–104.

[15] Y. Iwasa, D.C. Larbalestier, M. Okada, R. Penco, M.D. Sumption, X.X. Xi, A round table discussion on MgB_2 toward a wide market or a niche production? A summary, IEEE Transactions on Applied Superconductivity 16 (2) (2006) 1457–1464.

[16] H. Ullmaier, Irreversible Properties of Type II Superconductors, Springer-Verlag, Berlin, Heidelberg, New York, 1975.

[17] G. Blatter, M.V. Feigelman, V.B. Geshkenbein, A.I. Larkin, V.M. Vinokur, Vortices in high-temperature superconductors, Reviews of Modern Physics 66 (4) (1994) 1125–1388.

[18] M. Murakami, in: S. Jin (Ed.), Processing and Properties of High-T_c Materials, vol. 1, World Scientific, New Jersey, London, Hong Kong, 1993.

[19] F. Sandiumenge, B. Martinez, X. Obradors, Tailoring of microstructure and critical currents in directionally solidified $YBa_2Cu_3O_{7-x}$, Superconductor Science and Technology 10 (7A) (1997) A93–A119.

[20] K. Vinod, R.G.A. Kumar, U. Syamaprasad, Prospects for MgB_2 superconductors for magnet application, Superconductor Science and Technology 20 (1) (2007) R1–R13.

[21] C. Meingast, P.J. Lee, D.C. Larbalestier, Quantitative description of a high-J_c Nb–Ti superconductor during its final optimization strain 1. Microstructure, Tc, H_{c2}, and resistivity, Journal of Applied Physics 66 (12) (1989) 5962–5970.

[22] C. Meingast, D.C. Larbalestier, Quantitative description of a very high critical current-density Nb–Ti superconductor during its final optimization strain 2. Flux pinning mechanisms, Journal of Applied Physics 66 (12) (1989) 5971–5983.

[23] X.Y. Song, Z.J. Chen, S.I. Kim, D.M. Feldmann, D. Larbalestier, J. Reeves, Y.Y. Xie, V. Selvamanickam, Evidence for strong flux pinning by small, dense nanoprecipitates in a Sm-doped $YBa_2Cu_3O_{7-delta}$ coated conductor, Applied Physics Letters 88 (21) (2006).

[24] J. Jiang, B.J. Senkowicz, D.C. Larbalestier, E.E. Hellstrom, Influence of boron powder purification on the connectivity of bulk MgB_2, Superconductor Science and Technology 19 (8) (2006) L33–L36.

[25] S.K. Chen, M. Wei, J.L. MacManus-Driscoll, Strong pinning enhancement in MgB_2 using very small Dy_2O_3 additions, Applied Physics Letters 88 (19) (2006).

[26] K.A. Yates, Z. Lockman, A. Kursumovic, G. Burnell, N.A. Stelmashenko, J.L.M. Driscoll, M.G. Blamire, The effect of oxygenation on the superconducting properties of MgB_2 thin films, Applied Physics Letters 86 (2) (2005) 022502.

[27] S. Patnaik, L.D. Cooley, A. Gurevich, A.A. Polyanskii, J. Jing, X.Y. Cai, A.A. Squitieri, M.T. Naus, M.K. Lee, J.H. Choi, L. Belenky, S.D. Bu, J. Letteri, X. Song, D.G. Schlom, S.E. Babcock, C.B. Eom, E.E. Hellstrom, D.C. Larbalestier,

Electronic anisotropy, magnetic field-temperature phase diagram and their dependence on resistivity in *c*-axis oriented MgB_2 thin films, Superconductor Science and Technology 14 (6) (2001) 315–319.

[28] X.Y. Song, S.E. Babcock, C.B. Eom, D.C. Larbalestier, K.A. Regan, R.J. Cava, S.L. Bud'Ko, P.C. Canfield, D.K. Finnemore, Anisotropic grain morphology, crystallographic texture and their implications for flux pinning mechanisms in MgB_2 pellets, filaments and thin films, Superconductor Science and Technology 15 (4) (2002) 511–518.

[29] A. Gurevich, S. Patnaik, V. Braccini, K.H. Kim, C. Mielke, X. Song, L.D. Cooley, S.D. Bu, D.M. Kim, J.H. Choi, L.J. Belenky, J. Giencke, M.K. Lee, W. Tian, X.Q. Pan, A. Siri, E.E. Hellstrom, C.B. Eom, D.C. Larbalestier, Very high upper critical fields in MgB_2 produced by selective tuning of impurity scattering, Superconductor Science and Technology 17 (2) (2004) 278–286.

[30] X.Y. Song, V. Braccini, D.C. Larbalestier, Inter- and intragranular nanostructure and possible spinodal decomposition in low-resistivity bulk MgB_2 with varying critical fields, Journal of Materials Research 19 (8) (2004) 2245–2255.

[31] P. Kovac, I. Hugek, T. Meligek, J.C. Grivel, W. Pachla, V. Strbik, R. Diduszko, J. Homeyer, N.H. Andersen, The role of MgO content in ex situ MgB_2 wires, Superconductor Science and Technology 17 (10) (2004) L41–L46.

[32] B. Maiorov, S.A. Baily, H. Zhou, O. Ugurlu, J.A. Kennison, P.C. Dowden, T.G. Holesinger, S.R. Foltyn, L. Civale, Synergetic combination of different types of defect to optimize pinning landscape using $BaZrO_3$-doped $YBa_2Cu_3O_7$, Nature Materials 8 (5) (2009) 398–404.